INVENTIVE: A JOURNAL OF MULTIDISCIPLINARY STUDIES
Volume 4.(1), 21 January, 2022: *pp: 33-50*
Peer-Reviewed, Open Access - ISSN: 2773-7977 (Print); 2773-8183 (Online)

Geospatial approach on estimation and distribution of soil erosion using the RUSLE model. A case study of Ghorahi sub-metropolitan, Dang district.

Mahendra Singh Thapa*, Madhav Dhital
Institute of Forestry, Pokhara Campus, Pokhara, TU, Nepal.
*Corresponding Author's e-mail: msthapaiof@gmail.com

Received 8 November 2021, Reviewed 14 December 2021, Published 21 January 2022

Abstract
Soil erosion, involving the detachment and transport of soil particles, significantly degrades soil quality and reduces land productivity. The Chure region of Nepal faces severe land degradation primarily due to soil erosion, leading to declining agricultural yields, reservoir sedimentation, and groundwater depletion. This study aimed to assess soil erosion in Ghorahi Sub-Metropolitan City by generating thematic maps of erosion parameters and estimating the average annual soil loss using the Revised Universal Soil Loss Equation (RUSLE) in a GIS environment. Input data included precipitation records, soil maps, a digital elevation model (DEM), and Sentinel-2 satellite imagery. Six key factors rainfall-runoff erosivity (R), soil erodibility (K), slope length and steepness (LS), cover management (C), and support practices (P) were analyzed and integrated to model soil loss. Results indicated erosion rates ranging from 0 to 45.93 tons/ha/yr., with an average of 22.96 tons/ha/yr., exceeding national and regional benchmarks. Spatially, the northeastern and southern regions exhibited higher erosion susceptibility compared to the central-western areas. To mitigate erosion impacts, the study recommends land rehabilitation programs (afforestation, terracing), community engagement in conservation, bioengineering solutions, and improved road construction practices to minimize soil disturbance.

Keywords: *Soil erosion, RUSLE model, Sentinel-2, soil erodibility, rainfall erosivity, GIS, land degradation, Nepal*

Introduction
Soil represents a fundamental component of Earth's ecosystems, comprising a dynamic mixture of mineral particles, organic matter, water, air, and living organisms (Brady & Weil,

2016). This complex system supports essential ecological functions, agricultural productivity, and numerous industrial processes. However, anthropogenic activities including deforestation, intensive agriculture, and urbanization have significantly accelerated soil degradation worldwide (Lal, 2021), threatening these critical ecosystem services.

The global scale of soil erosion presents alarming challenges, with agricultural lands losing over 75 billion tons of soil annually (Pandey et al., 2009). Nepal's unique geographical characteristics - extreme topographic variation (60-8,848m), active tectonics, and concentrated monsoon rainfall (June-September) - make it particularly vulnerable to erosion processes (Chalise & Khanal, 1997). In mountainous ecosystems, soil erosion has emerged as a primary environmental concern (Nyssen et al., 2009), directly threatening food security through the loss of fertile topsoil (Morgan, 2009; Tesfahunegn et al., 2014). The environmental consequences of soil erosion extend far beyond agricultural impacts. This natural process of soil detachment and transport degrades land quality, reduces water quality through sedimentation, increases flood risks, and diminishes carbon sequestration capacity (Lal, 2014; Li et al., 2015; Six et al., 2019). Furthermore, erosion contributes to biodiversity loss and aquatic ecosystem degradation (Montgomery, 2017), creating complex environmental challenges.

The development of erosion modeling has evolved significantly since the introduction of the Universal Soil Loss Equation (USLE) by Wischmeier and Smith (1965). Subsequent advancements have produced more sophisticated tools including the Revised Universal Soil Loss Equation (RUSLE) (Renard et al., 1997), which incorporates improved algorithms for cover management, slope effects, and expanded climatic databases. These geospatial approaches now enable precise quantification and mapping of erosion patterns across landscapes.

Despite these technical advances, significant knowledge gaps remain regarding erosion impacts on forest ecosystems and local livelihoods. Effective soil conservation requires understanding community-level adaptation strategies and integrating local knowledge with scientific approaches. This study addresses these needs by investigating spatial patterns of soil erosion in Ghorahi Sub-Metropolitan City, Dang District, combining geospatial analysis with local ecological knowledge to inform sustainable land management practices.

Methods and Materials

Study Area

Ghorahi sub-metropolitan lies in the chure range of Lumbini province between 28°2' N latitude and 85°29' E longitude. It covers about 52221 ha with altitude around 600m above mean sea level. Ghorahi is mostly urban in central whereas rural areas are predominantly in North eastern of the region. Study area cover Ghorahi Sub-Metropolitan which possesses tropical and sub-tropical to the cool temperature type of climate. Ghorahi itself part of dun valley and is surrounded by chure hills in its three sides (north, south and east) and by the plain on the other central western part of region. The southern slopes of the northern hills are settled as well as cultivated whereas most of the northern slopes of the southern hills are covered with the natural vegetation. Central region is more urbanize and cultivated for agriculture.

Data Collection

This study mostly makes use of the secondary data. The data that were collected and acquired for this research purpose were:

Precipitation data

Precipitation data is required for the determination of the rainfall erosivity of the area. Hence, data of average annual precipitation of 10 years was obtained from the Department of Hydrology and Meteorology (DHM) of two stations located in Ratamata and Sukhabare.

Soil map

Soil and terrain (SOTER) database generated by Food and Agricultural Organization of the United Nations (FAO), the United Nations Environmental Programme and ISRIC, under the backings of the International Soil Science Society of scale 1;1 million map was used to serve the purpose of generation of the soil erodibility data.

ASTER Global Digital Elevation Model

ASTER Global DEM in TIFF format of the spatial resolution 30m was used which was downloaded from the website usgs.earthexplorer.gov

Figure 1

Map of the study area

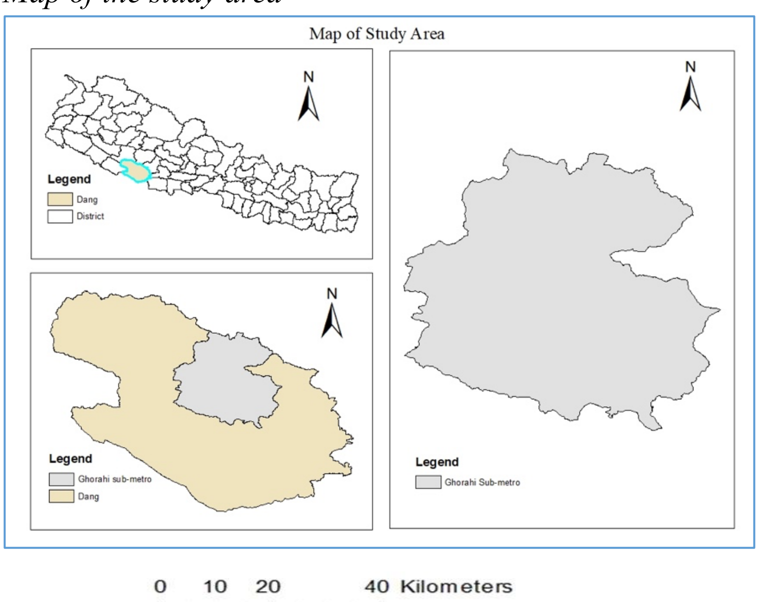

Satellite data

Satellite data was used for the preparation of the land use land cover map. Sentinal-2 image of date 2020/1/1 to 2021/1/1 was acquired from https://scihub.copernicus.eu/.

$A = R \times K \times LS \times C \times P$

Where:

dAi = average annual rate of soil loss (t/ha/yr.),

Ri= rainfall runoff erosivity factor (MJ mm ha-1h-1),

Ki = soil erodibility factor (t ha h ha-1 MJ-1 mm-1),

LS= Topographic Factor (Dimensionless),

Ci = crop or cover management factor (Dimensionless) and

Pi= conservation/support practice factor (Dimensionless) of the ith cell

After the generation of 6 input parameters, all of the factor maps were projected to UTM zone 44 and resampled to 30m of spatial resolution. All these maps were imported into ArcMap and the Raster Calculator tool within the spatial analyst extension was used to multiply all 6 parameters. The resulting map was composite soil erosion map showing average annual soil loss of the pixel. The average value of the whole watershed was found out using get raster properties tool excluding water bodies and built-up land.

Analysis

Generation of the Input Parameters

The Revised Universal Soil Loss Equation (RUSLE) estimates average annual soil loss using six key parameters: rainfall-runoff erosivity (R), soil erodibility (K), slope length and steepness (LS), cover management (C), and support practices (P). Below is the methodology applied to derive each parameter.

Rainfall-Runoff Erosivity Factor (R Factor)

The rainfall-runoff erosivity factor (R-factor), which quantifies the erosive potential of rainfall by combining raindrop kinetic energy with peak 30-minute intensity (EI_{30}) (Renard et al., 1997), was estimated using mean annual precipitation data due to limited high-resolution rainfall intensity measurements. For Himalayan conditions, the R-factor was calculated through a regression equation ($R = 79 + 0.363 \times P$) developed by Singh et al. (1981), where R represents the rainfall erosivity factor (MJ mm ha^{-1} hr^{-1} yr^{-1}) and P denotes mean annual precipitation (mm). The methodology involved collecting 10-year annual rainfall data from three meteorological stations within the catchment, spatially interpolating the precipitation values using the Inverse Distance Weighting (IDW) method in ArcGIS, and ultimately generating the R-factor map by applying the regression equation through the Raster Calculator tool in ArcMap. This approach provided a reliable estimation of rainfall erosivity across the study area while accounting for regional precipitation patterns.

Soil Erodibility Factor (K Factor)

The soil erodibility factor (K-factor), which quantifies a soil's inherent susceptibility to erosion under standard conditions (9% slope and 22.13 m plot length), was determined following a systematic methodology. The process began with soil data preparation, where a soil map of the study area was clipped and SOTER (Soil and Terrain Database) units were identified. Representative soil profiles were then extracted from available metadata, incorporating key soil properties including texture, organic matter content, and permeability. The K-factor values were calculated using the Erosion-Productivity Impact Model (EPIC) developed by Williams et al. (1990), which considers the percentage of sand, silt, and clay, organic matter content, soil structure, and permeability. Finally, these calculated K-values, ranging from 0 (indicating low erodibility) to 1 (representing highly erodible soils), were spatially assigned to their corresponding soil units to generate a comprehensive K-factor raster for the study area (Mhangara et al., 2012).

$K = F_{csand} * F_{si\text{-}cl} * F_{orgc} * F_{hisand} * 0.1317$

Fcsand= [0.2+0.3.exp (-0.256*Ms*(1-Msilt/100))],

Fcl-si= (Msilt/Mc+Msilt) ^0.3,

Forg C= (1-0.25orgC/orgC+exp (3.72-2.95*OrgC)),

Fhsand=(1-0.7(1-Ms/100)/(1-Ms/100) +exp(-5.51+22.9*(1-Ms/100))),

The resulting K value is reported in United States customary units of short ton · ac · h/ (100 ft · short ton · ac · in). After acquiring K values, it was attributed to respective SOTER units and rasterized using Polygon to Raster tool of ArcMap with cell size of 30m.

Topographic Factor (LS factor)

Topographic factor –Slope Length and Steepness (LS) is a combination of slope gradient factor (S) and a slope-length factor (L), which are determined from the DEM. Slope-length factor is a vital parameter in soil erosion modeling and computing transport capacity of surface runoff. An increase in the slope length of area indicates the steepness in which soil loss per unit area increases. The association of soil loss to terrain gradient is influenced by the vegetation coverage and soil particle size. It expresses the effect of topography, specifically hill slope length on erosion.

LS= Pow[(Flowaccum*cellsize/22.1,0.6) *pow(sin(slope*0.01745)/0.09,1.3] (Desalegn et al. 2018) …eq3

Crop Management Factor (C Factor)

The C-factor quantifies the influence of vegetation cover and land management practices on soil erosion rates. It ranges from 0 (maximum protection, e.g., dense forest) to 1 (bare soil with no protection) (Renard et al., 1997). Since vegetation cover reduces erosion by intercepting rainfall and stabilizing soil, accurate land use classification is essential for determining C-factor values (Gitas et al., 2009). The methodology for determining the Crop Management Factor (C-factor) involved several key steps. First, satellite imagery processing was conducted using a Sentinel-2 image (UTM Zone 44) with acquisition dates spanning 2020 to 2021. Next, land use/land cover (LULC) mapping was performed by applying a Random Forest classifier to categorize the study area into four distinct classes: water bodies, settlements, agricultural land, and forested areas. Following classification, the LULC map was converted to vector format, where polygons representing the same land cover class were merged, and appropriate C-factor values from existing literature were assigned to each land cover type. Finally, the vector data was converted back to a 30-meter resolution raster format using the Polygon to Raster tool in ArcGIS to facilitate further spatial analysis and integration with other RUSLE parameters.

Conservation/Support Practice Factor (P Factor)

The P-factor reflects the impact of soil conservation measures (e.g., contour farming, terracing) on reducing erosion by altering runoff flow patterns (Renard & Foster, 1983). The methodology for determining the Conservation/Support Practice Factor (P-factor) involved two primary steps. First, the previously classified Land Use/Land Cover (LULC) map was converted to a vector format, and appropriate P-values derived from existing literature were systematically assigned to each land use type. Subsequently, the vector data was transformed into a P-factor raster layer to facilitate seamless integration with the other RUSLE parameters in the soil erosion modeling process. This approach ensured consistent representation of conservation practice effects across different land use categories within the study area.

2.3.2 Assessment of annual rate of soil erosion

RUSLE equation was used to determine average annual soil loss of the study area. The RUSLE equation for estimation of average annual rate of soil erosion is expressed as:

$A = R \times K \times LS \times C \times P$

Where,

A = average annual rate of soil loss (t/ha/yr),

R rainfall runoff erosivity factor (MJ mm ha-1 h -1),

K= soil erodibility factor (t ha h ha-1 MJ-1 mm-1),

LS =Topographic factor (Dimensionless),

C= crop or cover management factor (Dimensionless) and

P= conservation/support practice factor (Dimensionless)

After the generation of 6 input parameters, all of the factor maps were projected to UTM zone 44 and resampled to 30m of spatial resolution. All these maps were imported into ArcMap and Raster Calculator tool within spatial analyst extension was used to multiply all 6 parameters. The resulting map was composite soil erosion map showing average annual soil loss of the pixel. The average value of the whole watershed was found out using get raster properties tool excluding water bodies and built-up land.

RESULTS AND DISCUSSION

Input parameters of RUSLE

Rainfall Runoff Erosivity Factor

The rainfall erosivity factor quantifies the effect of rainfall impact and also reflects the amount and rate of runoff likely to be associated with precipitation events (Xu et al., 2008). Since there was insufficient rainfall record, regression equation linking annual precipitation data to R factor was used. The average annual precipitation data of 10 years of the stations that were used were:

Table 1

Annual Rainfall Data of Various Rainfall Stations

Station	Latitude	Longitude	Precipitation	Erosivity
Sukhabare	28.015945	82.390795	103.9221212	116.724
Ratamata	27.96281694	82.61207	144.4979389	120.563

The precipitation values were interpolated using inverse distance weighting method over the whole watershed. Then, the regression equation $R = 79 + 0.363\times P$ where P is the precipitation value and R are the R factor value used. The R factor value ranged from 116.724 to 120.563MJ mm ha-1 hr-1 year-1 over the whole Ghorahi sub-metropolitan.

Soil Erodibility Factor

For determining the K factor, soil map was used. The different type of soil texture that were present in the study area were silt clay loam, loam, sandy loam and silt loam with SOTER. Using EPIC model as described in the methodology earlier, the required parameters required for the model were selected. Percent sand, silt and clay of only upper horizon was selected assuming that soil is eroded from the upper horizon and since the metadata only had percent organic matter but the model requires percent carbon, standard assumption that 58% of the total organic matter is carbon was used. The resulting K value is reported in United States customary units of short ton · ac · h/ (100 ft · short ton · ac · in) which was multiplied by conversion factor of 0.1317 to obtain result in SI units of t.ha.h/(ha.MJ.mm).

Table 2

Soil Erodibility Values for Different Soil Textures

Soil unit symbol	Sand % topsoil	Silt % topsoil	Clay % topsoil	OC % topsoil	K value
TH	41	41.3	17.7	7.03	0.017804
TM	31.2	39.6	29.2	3.95	0.01694
LV	26.1	27.3	46.7	1.86	0.015091
LP	69.9	10.5	19.5	0.73	0.017397

LD	42.02	29.67	28.27	3.39	0.016617

Topographic Factor

Factor L was computed using DEM as an input source with the methodology applied as mentioned above. Slope map and flow accumulation map were derived from DEM so as to compute LS factor. Raw DEM was filled to fill any sinks or imperfection in the data after which elevation of the study area ranged from 787 to 2413m. The slope calculated in degree ranged from 0 to 66.6157 20 degree whereas flow accumulation value ranged from 0 to 295563 which was derived from flow direction raster calculated from DEM. For the intermediate factors required for calculating factor L and slope gradient S is calculated by Rater calculator. Finally factor LS was obtained ranging from 0 to 187.85.

Crop Management Factor

For deriving C factor map, LULC map of the watershed was created initially.

LULC condition of Ghorahi

For the land use land cover calculation sentinel-2 image is used with random forest algorithms for the classification of land cover. The LULC classes that were selected were forest area, agricultural land, settlement and water bodies. While looking at LULC map, it is clear that northern and eastern as well as southern side of the Ghorahi is mostly has mainly forest land with few agriculture sites with contour farming whereas the central portion of Ghorahi is practiced agriculture and settled heavily. Forest on the southern side is in small patches and most of them are open type forest and degraded whereas north eastern forest is mostly dense forest. The urban area is mostly concentrated on the central and western part of Ghorahi. Barren lands are mostly found on the sand shore area of the streams contributing to the watershed. So, the barren land around the watershed is more prone for the soil erosion and cumulated for soil loss.

Table 3

Accuracy Assessment of LULC Of Ghorahi sub-metropolitan

Class	Producer accuracy	User Accuracy
Forest	92.85	90.69
Water	100	97.43
Settlement	95.65	91.66
Agriculture	87.8	94.73
Overall accuracy	93.75	
Kappa	0.91	

The kappa coefficient of land use land cover image was 0.91 which is close to 1 meaning there is 91% of agreement than chance alone.

C factor values according to land use were referenced from literature consultation. The land classes were converted to vector file and C factor values were attributed in the attribute table. Then it was again converted to raster file with the cell size of 30. The prescribed C factor values were:

Table 4

C factor value for crop management factor

Land class	C factor value
Water body	0
Settlement	0.003
Agriculture	0.15
Forest	0.01

Conservation/Support practice factor

Conservation or support practice factor (P) is the ratio between soil loss with a specific support practice and the corresponding loss with up and down slope tillage. These conservation practices dominantly affect erosion by improving the flow pattern, grade, or direction of surface runoff and reducing the amount of rate of runoff. P-value ranges from 0 to 1, where the value 0 indicates good erosion resistant facility made by man and the value 1 indicate an absence of erosion resistant facility. The P factor values prescribed to different land classes were:

Table 5

P factor according to slope

Slope	P factor value
0-7	0.55
7-11.3	0.6
11.3-17.6	0.8
17.6-26.8	0.9
26.8>	1

(Koirala et al 2019)

Figure 2

Rainfall Runoff Erosivity Factor Map

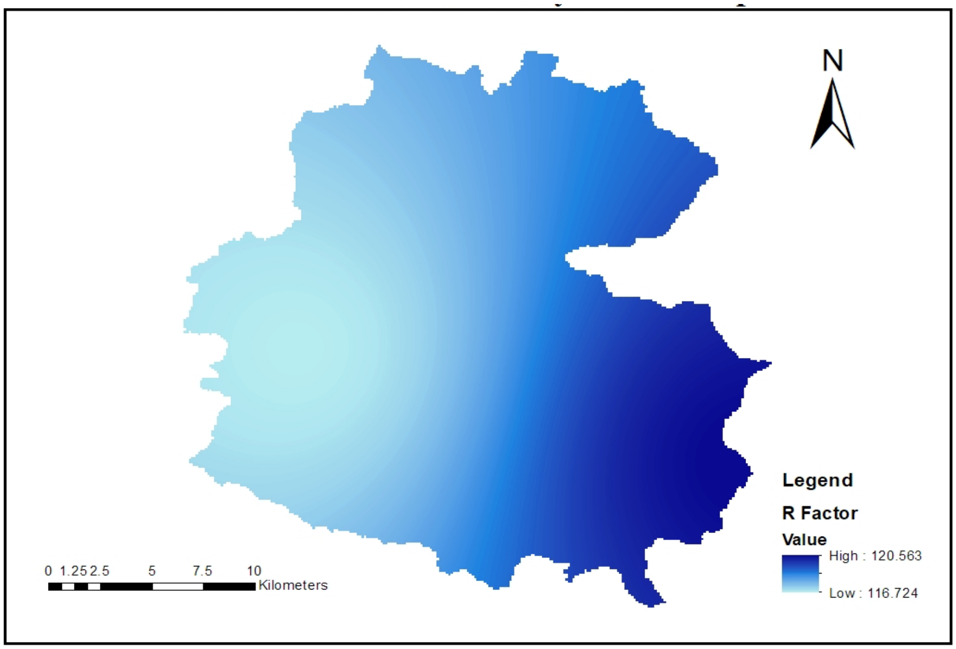

Figure 3

Soil erodibility factor map

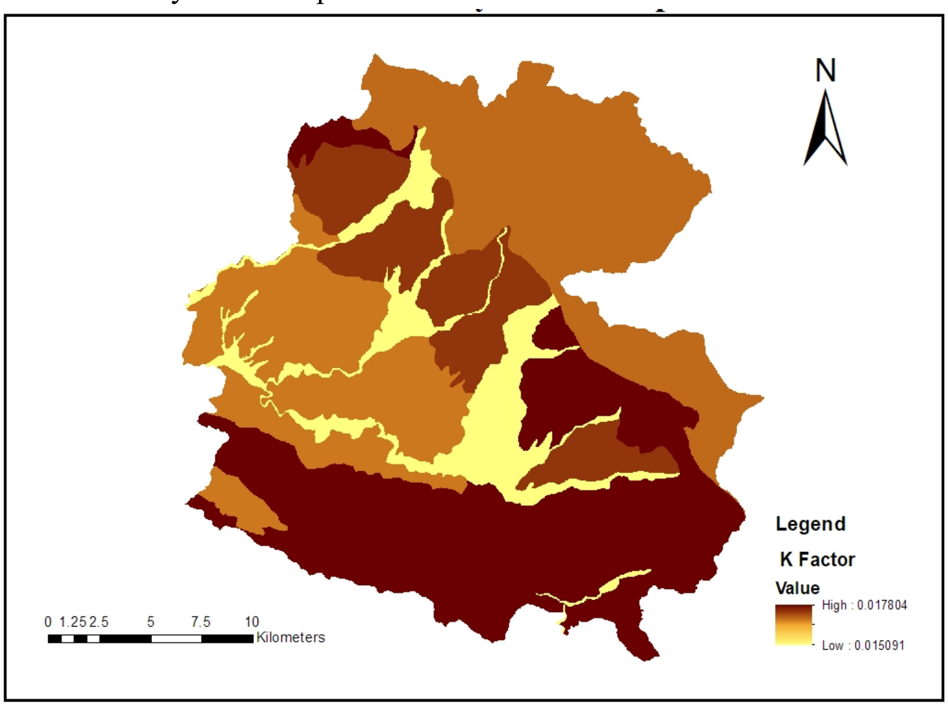

Figure 4

Topographic Factor map

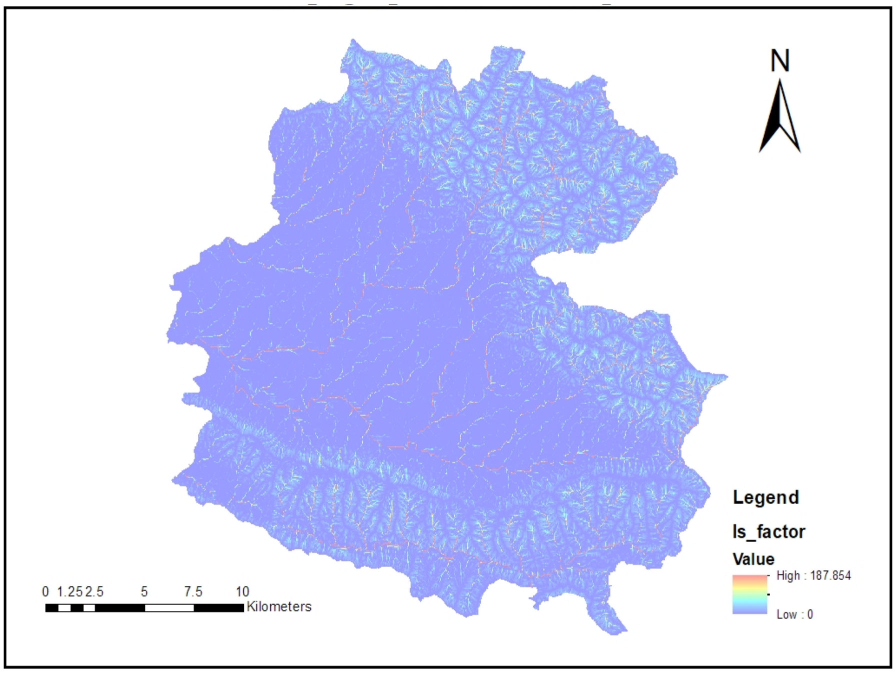

Figure 5
Crop Management Factor Map

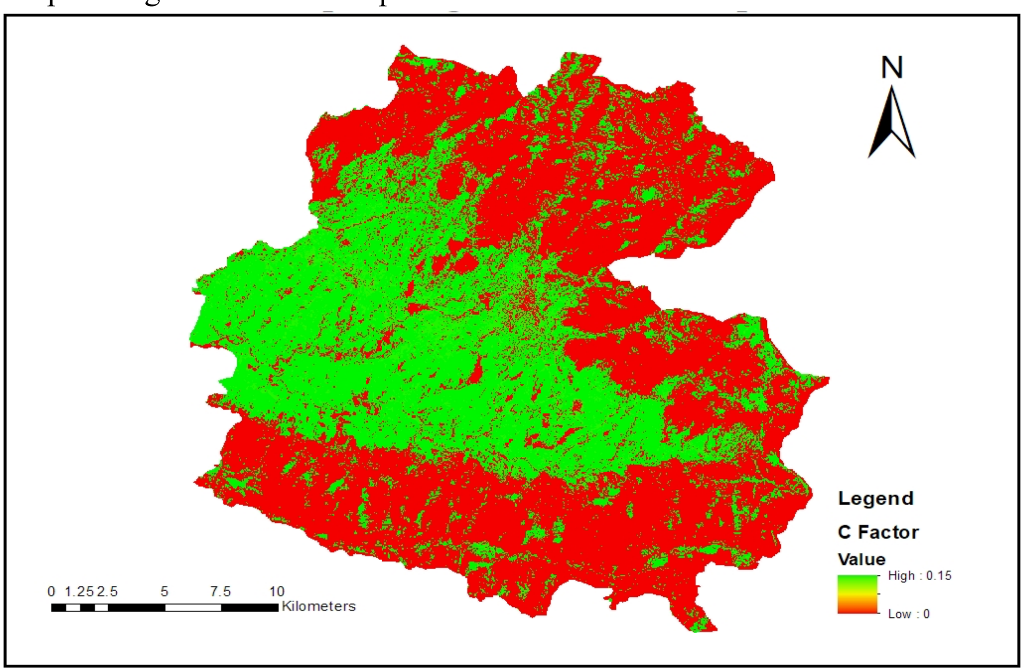

Figure 6
Support Practice Factor Map

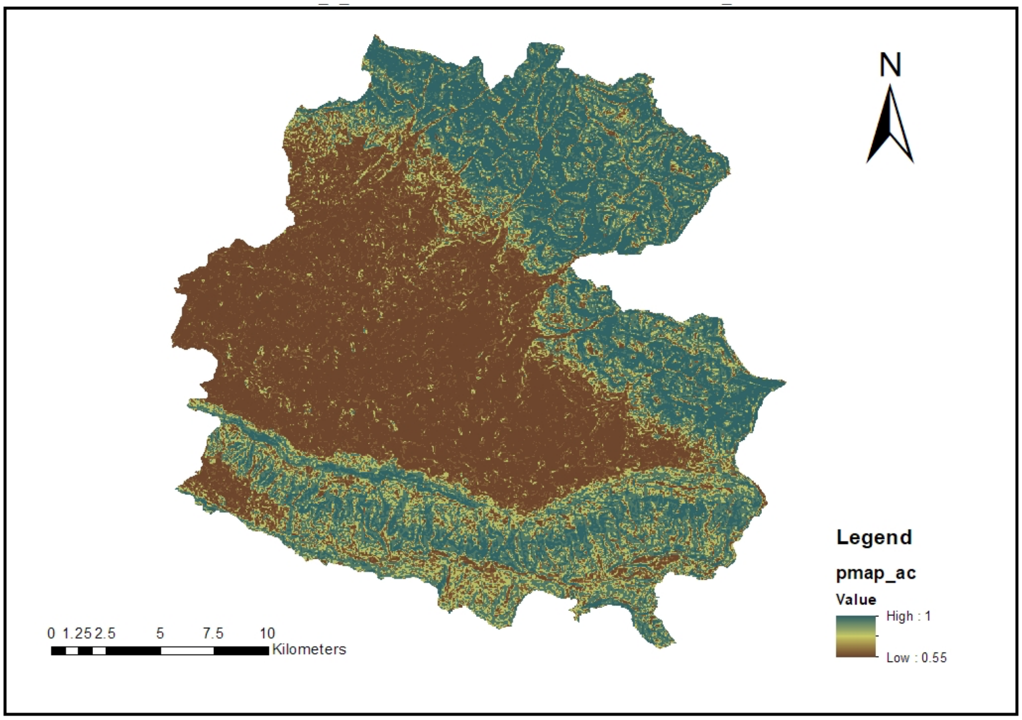

Erosion Rate in the Study Area

After obtaining 6 parameters of the RUSLE equation, all the factors were projected to the UTM 44 projection system and pixel size of each thematic layers were resampled to the 30m*30m. Raster calculator on ArcMap > Spatial Analyst Tools > Map Algebra > Raster calculator was used to multiply all those 6 factors. The final result obtained was:

Table 6

Erosion rate in the study area

Value field	Results
Minimum rate	0 Tons/hectare/year
Maximum rate	45.93 Tons/hectare/year
Average rate	22.96 Tons/hectare/year

The final soil erosion composite map obtained is presented in figure 7.

Figure 7

Composite Soil loss map

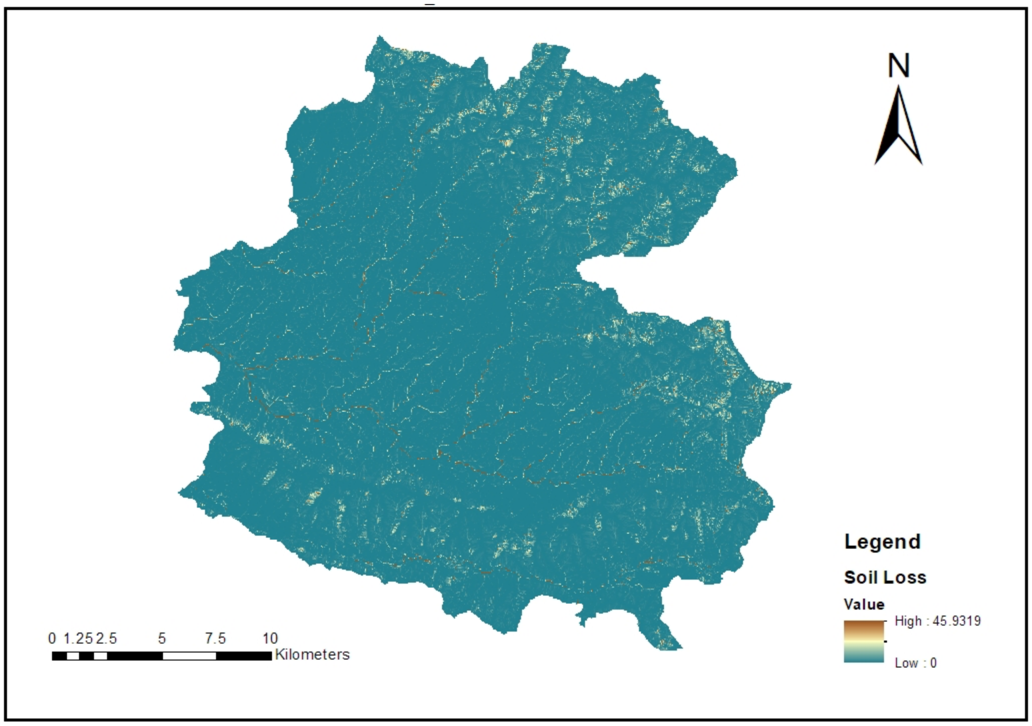

As evident from the map, most of the areas with soil erosion were located on the north eastern and southern side of the watershed whereas most of the low risk of soil erosion was on the western part /central region of the watershed, as it is mostly forested. Since no distinction was made between open forest and dense forest due to relatively coarser resolution of the dataset, both dense and open forest were given very low C factor values resulting in most of the forest areas of the whole watershed with low probability of soil erosion. Likewise, areas of low and moderate intensity of soil erosion were mostly located in the agricultural lands all around the watershed with having less steep topography influenced by low L and S factor. High intensity of soil erosion was also mostly located in the agricultural lands with steep topography. Likewise, pixels of water bodies classes were clustered together mostly along barren lands with their location mentioned as above in erosion hotspots.

Very few studies have been done in soil loss around the Chure in regards to soil erosion despite it being a serious problem in the Chure. When considering recent studies, Koirala et al (2019) used RUSLE model to calculate soil erosion rate of High Mountains, High Himal, Chure, and Terai have mean erosion rates of 38.0, 32.0, 28.0, 7.0, and 0.1 t ha−1 yr respectively with annual soil loss rate 25 t ha−1 yr−1. It is clear that the difference in model makes considerable difference in estimation of the soil erosion since each model requires difference input parameters. Hence, it is evident that soil loss calculation using several models accompanied by locally relevant field-based calculations to compare and approximate the results to gain the clearer understanding of the erosion process in Ghorahi is crucial.

CONCLUSION AND RECOMMENDATIONS

The study evaluated soil erosion in the Ghorahi sub-metropolitan area using precipitation data, soil maps, DEM, and satellite imagery, identifying six key parameters influencing erosion. The average soil erosion rate was found to be 22.96 ton/ha/yr, significantly higher than the national average (25 ton/ha/yr) and the Chure range (7 ton/ha/yr). Barren areas near water bodies were most susceptible, followed by agricultural land, while forested regions showed the least erosion. The southern and northeastern parts of the watershed were more erosion-prone compared to the central area. To mitigate soil loss, land rehabilitation programs such as afforestation and terracing should be prioritized, especially on steep slopes and sparsely vegetated areas. Additionally, raising community awareness on sustainable land use and involving local stakeholders in conservation efforts is essential. Implementing low-cost bioengineering techniques and ensuring proper soil conservation measures during rural road construction will further reduce erosion risks. These measures will support sustainable land management and long-term environmental stability in the region.

References

Adhikari, P., Nejadhashemi, A. P., & Woznicki, S. A. (2017). Soil erosion assessment and its impact on the livelihood of smallholder farmers in the eastern Himalayas: A case study in Nepal. *Environmental Monitoring and Assessment, 189*(8), 408. https://doi.org/10.1007/s10661-017-6136-7

Alkharabsheh, M., Alexandridis, T., Bilas, G., Misopolinos, N., & Silleos, N. (2013). Impact of land cover change on soil erosion hazard in northern Jordan using remote sensing and GIS. *Procedia Environmental Sciences, 19*, 912–921. https://doi.org/10.1016/j.proenv.2013.06.101.

Al-Seekh, S. H., & Mohammad, A. G. (2009). The effect of water harvesting techniques on runoff, sedimentation, and soil properties. *Environmental Management, 44*(1), 37–45. https://doi.org/10.1007/s00267-009-9310-z.

Ashiagbor, G., Forkuo, E. K., Laari, P., & Aabeyir, R. (2012). Modeling soil erosion using RUSLE and GIS tools. *International Journal of Remote Sensing & Geoscience, 2*(1), 7–17.

Assouline, S., & Ben-Hur, M. (2006). Effects of rainfall intensity and slope gradient on the dynamics of interrill erosion during soil surface sealing. *Catena, 66*(3), 211–220. https://doi.org/10.1016/j.catena.2006.02.005.

Atoma, H., Suryabhagavan, K. V., & Balakrishnan, M. (2020). Soil erosion assessment using RUSLE model and GIS in Huluka watershed, Central Ethiopia. *Sustainable Water Resources Management, 6*(1). https://doi.org/10.1007/s40899-020-00365-z.

Atreya, K., Sharma, S., Bajracharya, R. M., & Rajbhandari, N. P. (2006). Applications of reduced tillage in hills of central Nepal. *Soil and Tillage Research, 88*(1–2), 16–29. https://doi.org/10.1016/j.still.2005.04.003.

Bajracharya, A. R., Bajracharya, S. R., Shrestha, A. B., & Maharjan, S. B. (2018). Climate change impact assessment on the hydrological regime of the Kaligandaki Basin, Nepal. *Science of the Total Environment, 625*, 837–848. https://doi.org/10.1016/j.scitotenv.2017.12.332.

Bhandari, K. P., Aryal, J., & Darnsawasdi, R. (2015). A geospatial approach to assessing soil erosion in a watershed by integrating socio-economic determinants and the RUSLE model. *Natural Hazards, 75*, 321–342. https://doi.org/10.1007/s11069-014-1321-2.

Bruijnzeel, L. A. (2004). Hydrological functions of tropical forests: Not seeing the soil for the trees? *Agriculture, Ecosystems & Environment, 104*(1), 185–228. https://doi.org/10.1016/j.agee.2004.01.015.

Chadli, K. (2016). Estimation of soil loss using RUSLE model for Sebou watershed (Morocco). *Modeling Earth Systems and Environment, 2*(2), 1–10. https://doi.org/10.1007/s40808-016-0105-y.

Chalise, D., & Kumar, L. (2020). Land use change affects water erosion in the Nepal Himalayas. *PLOS ONE, 15*(4), e0231692. https://doi.org/10.1371/journal.pone.0231692

Chalise, D., Kumar, L., Sharma, R., & Kristiansen, P. (2020). Assessing the impacts of tillage and mulch on soil erosion and corn yield. *Agronomy, 10*(1), 63. https://doi.org/10.3390/agronomy10010063

Chalise, D., Kumar, L., Shriwastav, C. P., & Lamichhane, S. (2018). Spatial assessment of soil erosion in a hilly watershed of Western Nepal. *Environmental Earth Sciences, 77*(19). https://doi.org/10.1007/s12665-018-7842-3.

Desalegn, A., Tezera, A., & Tesfay, F. (2018). Developing GIS-based soil erosion map using RUSLE of Andit Tid Watershed, Central Highlands of Ethiopia. *Journal of Scientific Research and Reports, 19*(1), 1–13. https://doi.org/10.9734/jsrr/2018/40841

Devatha, C. P., Deshpande, V., & Renukaprasad, M. S. (2015). Estimation of soil loss using USLE model for Kulhan Watershed, Chattisgarh—A case study. *Aquatic Procedia, 4*, 1429–1436. https://doi.org/10.1016/j.aqpro.2015.02.185.

Efthimiou, N., Lykoudi, E., & Karavitis, C. (2014). Soil erosion assessment using the RUSLE model and GIS. *European Water, 47*, 15–30.

Food and Agriculture Organization (FAO). (2015). *Status of the world's soil resources*. FAO. https://doi.org/10.978-92-5-109004-6.

Ganasri, B. P., & Ramesh, H. (2016). Assessment of soil erosion by RUSLE model using remote sensing and GIS—A case study of Nethravathi Basin. *Geoscience Frontiers, 7*(6), 953–961. https://doi.org/10.1016/j.gsf.2015.10.007.

Govers, G., Merckx, R., Van Wesemael, B., & Van Oost, K. (2017). Soil conservation in the 21st century: Why we need smart agricultural intensification. *Soil, 3*(1), 45–59. https://doi.org/10.5194/soil-3-45-2017.

Gurung, S. (2021). Soil erosion status of Nepal. *Nepalese Journal of Environmental Science, 8*(1–2), 1–10. https://doi.org/10.3126/nutaj.v8i1-2.44109.

Karamage, F., Shao, H., Chen, X., Ndayisaba, F., Nahayo, L., Kayiranga, A., et al. (2016). Deforestation effects on soil erosion in the Lake Kivu Basin, D.R. Congo-Rwanda. *Forests, 7*(11), 281. https://doi.org/10.3390/f7110281.

Koirala, P., Thakuri, S., Joshi, S., & Chauhan, R. (2019). Estimation of soil erosion in Nepal using a RUSLE modeling and geospatial tool. *Geosciences, 9*(4), 147. https://doi.org/10.3390/geosciences9040147.

Krishna Bahadur, K. C. (2012). Spatio-temporal patterns of agricultural expansion and its effect on watershed degradation: A case from the mountains of Nepal. *Environmental Earth Sciences, 65*(7), 2063–2077. https://doi.org/10.1007/s12665-011-1186-6.

Li, Z., & Fang, H. (2016). Impacts of climate change on water erosion: A review. *Earth-Science Reviews, 163*, 94–117. https://doi.org/10.1016/j.earscirev.2016.10.004.

Lufafa, A., Tenywa, M. M., Isabirye, M., Majaliwa, M. J. G., & Woomer, P. L. (2003). Prediction of soil erosion in a Lake Victoria basin catchment using a GIS-based Universal Soil Loss model. *Agricultural Systems, 76*(3), 883–894. https://doi.org/10.1016/S0308-521X(02)00012-4.

Montanarella, L., Pennock, D. J., McKenzie, N., Badraoui, M., Chude, V., Baptista, I., et al. (2015). World's soils are under threat. *SOIL Discussions, 2*(2), 1263–1272. https://doi.org/10.5194/soild-2-1263-2015.

Navas, A., Valero Garcés, B., & Machín, J. (2004). An approach to integrated assessment of reservoir siltation: The Joaquín Costa reservoir as a case study. *Hydrology and Earth System Sciences, 8*(6), 1193–1199. https://doi.org/10.5194/hess-8-1193-2004.

Nehai, S. A., Guettouche, M. S., & Saadoud, D. (2020). Regional modeling of soil sensitivity to water erosion in JIJEL region (Algeria) using MCA and GIS. *Applied Geomatics, 12*(3), 301–314. https://doi.org/10.1007/s12518-020-00316-5.

Nkonya, E., Phillip, D., Mogues, T., Pender, J., Oni, O., Kato, E., & Simeon, E. (2016). From land use to land cover: Restoring the environmental services of degraded lands in developing countries. *World Bank.*

Panagos, P., Borrelli, P., Meusburger, K., Alewell, C., Lugato, E., & Montanarella, L. (2015). Estimating the soil erosion cover-management factor at the European scale. *Land Use Policy, 48*, 38–50. https://doi.org/10.1016/j.landusepol.2015.05.021.

Pardhan, B., Yusoff, I., & Jafri, M. Z. M. (2011). Soil erosion assessment and its correlation with landslide events using remote sensing data and GIS: A case study at Penang Island, Malaysia. *Environmental Monitoring and Assessment, 184*(2), 715–727. https://doi.org/10.1007/s10661-011-1996-8.

Prasannakumar, V., Vijith, H., Abinod, S., & Geetha, N. (2012). Estimation of soil erosion risk within a small mountainous sub-watershed in Kerala, India, using Revised Universal Soil Loss Equation (RUSLE) and geo-information technology. *Geoscience Frontiers, 3*(2), 209–215. https://doi.org/10.1016/j.gsf.2011.11.003.

Renard, K. G., Foster, G. R., Weesies, G. A., McCool, D. K., & Yoder, D. C. (1997). *Predicting soil erosion by water: A guide to conservation planning with the Revised Universal Soil Loss Equation (RUSLE)*. USDA.

Sato, Y., Ikeda, M., & Yamashita, O. (1994). Neurosecretory cells expressing the gene for common precursor for diapause hormone and pheromone biosynthesis activating neuropeptide in the suboesophageal ganglion of the silkworm, Bombyx mori. *General and Comparative Endocrinology, 96*(1), 27–36. https://doi.org/10.1006/gcen.1994.1156.

Shaikh, M. S., & Shetkar, R. V. (2018). Soil erosion estimation modelling by Revised Universal Soil Loss Equation and Soil and Water Assessment Tool on Geographic Information System platform. *International Journal of Engineering Research & Technology, 7*(10), 1–5.

Shrestha, D. P., Zinck, J. A., & Van Ranst, E. (2004). Modelling land degradation in the Nepalese Himalaya. *Catena, 57*(2), 135–156. https://doi.org/10.1016/j.catena.2003.11.003.

Tamene, L., & Vlek, P. L. G. (2008). Soil erosion studies in Northern Ethiopia. In A. K. Braimoh & P. L. G. Vlek (Eds.), *Land use and soil resources* (pp. 73–100). Springer. https://doi.org/10.1007/978-1-4020-6778-5_5.

Teshome, A., & Mekonnen, K. (2020). Soil erosion impact on livelihoods: Evidence from the highlands of Ethiopia. *Environmental Systems Research, 9*(1), 14. https://doi.org/10.1186/s40068-020-00177-2

Thapa, P. (2020). Spatial estimation of soil erosion using RUSLE modeling: A case study of Dolakha district, Nepal. *Environmental Systems Research, 9*(1), 15. https://doi.org/10.1186/s40068-020-00177-2.

Tolessa, T., Senbeta, F., & Kidane, M. (2017). The impact of land use/land cover change on ecosystem services in the central highlands of Ethiopia. *Ecosystem Services, 23*, 47–54. https://doi.org/10.1016/j.ecoser.2016.11.010.

Vatandaşlar, C., & Yavuz, M. (2017). Modeling cover management factor of RUSLE using very high-resolution satellite imagery in a semiarid watershed. *Environmental Earth Sciences, 76*(2). https://doi.org/10.1007/s12665-017-6388-0.

Wawer, R., Nowocień, E., & Podolski, B. (2005). Real and calculated soil erodibility factor (K-USLE) for some Polish soils. *Polish Journal of Environmental Studies, 14*(5), 655–658.

Weil, R. R., & Brady, N. C. (2017). *The nature and properties of soils* (15th ed.). Pearson.

Zewdie, S., Singh, B. R., & Lal, R. (2018). Impacts of soil erosion on soil fertility and crop productivity in the Ethiopian highlands: A review. *Land Degradation & Development, 29*(5), 1507–1522. https://doi.org/10.1002/ldr.2942.

***